Geomorphology 205 (2014) 120–127

Contents lists available at ScienceDirect

Geomorphology

journal homepage: www.elsevier.com/locate/geomorph

Impact of flow regulation on near-channel floodplain sedimentation

C.E. Renshaw [a,*], K. Abengoza [a], F.J. Magilligan [b], W.B. Dade [a], J.D. Landis [a]

[a] Department of Earth Sciences, Dartmouth College, Hanover, NH 03755, USA
[b] Department of Geography, Dartmouth College, Hanover, NH 03755, USA

ARTICLE INFO

Article history:
Received 8 August 2011
Received in revised form 19 July 2012
Accepted 8 March 2013
Available online 21 March 2013

Keywords:
Floodplains
Sedimentation
Flow regulation
Radionuclides

ABSTRACT

Rates and the spatial extent of near-channel floodplain sedimentation on regulated and unregulated reaches in two upland rivers in central Vermont, U.S.A. are measured using the short-lived fallout radionuclide ^{210}Pb. We find consistent profiles of ^{210}Pb inventories across all sites; inventories are low immediately next to the channel, increase to a peak value as the inundation frequency decreases and then asymptotically diminish with distance from the channel to the equilibrium inventory associated with atmospheric deposition alone. We infer from our data that flow regulation has impacted sediment deposition to floodplains below the dam; total sediment deposition is less and it is constrained to a narrower band immediately along the active channel. Flow regulation does not appear, however, to impact the general form of the ^{210}Pb inventory profile, suggesting a uniformity of process across regulated and unregulated floodplains.

1. Introduction

We use short-lived fallout radionuclides to compare the rates and spatial extent of floodplain sedimentation between regulated and unregulated reaches in two upland rivers in central Vermont, U.S.A. The White River is the longest unregulated river in New England while flow in the West River has been regulated by two flood-control dams since the early 1960s. Short-lived fallout radionuclides have been increasingly used to quantify decadal-scale floodplain sedimentation rates across a range of climatic environments (e.g., Humphries et al., 2010; Saint-Laurent et al., 2010). This study thus represents an extension of these important, earlier efforts to the specific question of the impact of flow regulation on floodplain sedimentation. We use the short-lived fallout radionuclide ^{210}Pb because its half-life (22.3 years) is similar to the timescale over which flow has been regulated on the West River.

A focus on floodplain dynamics is timely and pressing. More than 40% of the total organic carbon transported from the land to the oceans is in particulate form via rivers (Ludwig et al., 1996) and as much as half of the annual sediment load of a river is deposited on its floodplain (Lambert and Walling, 1987; Mertes, 1994; Walling and Owens, 2003; Bourgoin et al., 2007; Day et al., 2008). Sediment storage on floodplains thus has significant implications for global nutrient cycling (Walling and Fang, 2003) and for local transport and storage of sediment-associated nutrients and contaminants (Walling et al., 2003). Floodplain sedimentation also directly impacts the productivity and floristic assemblage of riparian ecosystems (Bornette et al., 1998; Steiger et al., 2005; Walls et al., 2005; Lowe et al., 2010) which are among the most diverse and productive ecosystems on Earth (Whited et al., 2007). For example, Cavalcanti and Lockaby (2005) found that root productivity declined sharply with floodplain sedimentation rates as low as 3 mm a^{-1}. Floodplain sedimentation also serves as an important mechanism of recurring ecological disruption which can directly enhance ecological diversity (Grime, 1973; Connell, 1978).

While it has been estimated that flow regulation by dams has significantly reduced the flux of sediment to the world's oceans (Walling and Fang, 2003), the extent to which flow regulation impacts sediment flux at reach scales (e.g. floodplain sedimentation) has not been quantified. Sediment impoundment behind dams results in an imbalance between sediment supply and transport capacity downstream of dams, which has been shown to lead to channel incision (Andrews, 1986; Vericat and Batalla, 2005; Surian and Cisotto, 2007) and narrowing of the bankfull channel width (Andrews, 1986; Friedman et al., 1998; Allred and Schmidt, 1999; Surian, 1999; Gaeuman et al., 2005; Grams et al., 2007). Loss of recurring inundation and deposition of fresh sediment on a floodplain owing to river regulation results in subsequent revegetation and the development of new, lower terraces on a floodplain that can further reduce channel width (Petts, 1984; Grams and Schmidt, 2002; Magilligan and Nislow, 2005; Curtis et al., 2010). Evacuation of fine sediment associated with channel incision may also lead to sandbar erosion (Grams et al., 2007) and decreased embeddedness (Salant et al., 2006). Collectively, these effects suggest significant, regulation-induced changes to overbank sedimentation and the associated rates and extent of the exchange of nutrients between a channel and its floodplain (Thoms, 2003). As attempts to re-establish the ecological connectivity (Ward, 1998) of upland river floodplains in regulated systems gain popularity (Debano and Schmidt, 1990), there is a growing need for a more thorough understanding of the natural functioning of upland riparian ecosystems, and the sediment and nutrient dynamics in these settings (Henry and Amoros, 1995; Stanford et al., 1996; Ward et al., 2001).

* Corresponding author. Tel.: +1 603 646 3365; fax: +1 603 646 3922.
E-mail address: Carl.E.Renshaw@Dartmouth.edu (C.E. Renshaw).

0169-555X/$ – see front matter © 2013 Elsevier B.V. All rights reserved.
http://dx.doi.org/10.1016/j.geomorph.2013.03.009

The overall goal of this research is to provide a greater understanding of the processes governing the near-channel spatial variation in floodplain sedimentation. We develop a field-tested conceptual model developed from ^{210}Pb inventories and sediment deposition that links inundation frequency to the spatial pattern and rate of floodplain sedimentation. Moreover, we apply this model to both regulated and unregulated stream systems to document the effect of flow regulation on riverine-floodplain connectivity.

2. Floodplain inventories

Along any given reach, Pizzuto (1987) hypothesized that the rate of overbank sediment deposition decays exponentially with increasing distance from the channel due to the dispersion of turbulent energy across the floodplain. Initial attempts to rigorously test the validity of this hypothesis were limited by the lack of quantitative sediment deposition data with sufficient temporal resolution. However, with the advent of radionuclide-based techniques for quantifying sedimentation rates (He and Walling, 1996; Walling and He, 1997), the number and quality of floodplain sedimentation-rate measurements have increased dramatically over the last decade. Results from radionuclide-based measurements of the spatial variation in lowland floodplain sedimentation have generally found the proposed decay in deposition with increasing distance from the channel, although the rate of decay and the specific mechanisms controlling this decay remain uncertain (Asselman and Middelkoop, 1995; Tornqvist and Bridge, 2002; Nicholas and Mitchell, 2003; Day et al., 2008; Pizzuto et al., 2008).

Our work extends these earlier studies by explicitly investigating the impact of flow regulation on the pattern of floodplain sedimentation. To do this, we use the fallout radionuclide ^{210}Pb to estimate floodplain sedimentation rates. ^{210}Pb is one of several short-lived intermediates in the ^{238}U decay series that can be written in abridged form as

$$^{238}\mathrm{U}\rightarrow{}^{226}\mathrm{Ra}\rightarrow{}^{222}\mathrm{Rn}\rightarrow{}^{210}\mathrm{Pb}\rightarrow{}^{206}\mathrm{Pb}.$$

^{238}U has a long half-life ($t_{1/2}$ = 4.5 billion years), and as a consequence, its decay acts as a pseudocontinuous source of ^{226}Ra. Thus, in a closed system all the daughters of ^{238}U decay will be in secular equilibrium, defined as each daughter element having the same activity, $n\lambda$, where n is the number of atoms present and λ is their decay constant.

In near surface sediments and soils, gaseous ^{222}Rn ($t_{1/2}$ = 3.8 days) partially diffuses to the atmosphere where it subsequently decays to ^{210}Pb and returns to the surface as atmospheric fallout, primarily by wet deposition (Appleby and Oldfield, 1992). While there is significant variation in ^{210}Pb deposition rates over short timescales, mean annual deposition at a given location is relatively constant from year to year (Appleby, 2008). ^{210}Pb is highly surface reactive and quickly sorbs onto particles (Kaste et al., 2003). Thus, in near-surface soils and sediments, atmospheric deposition of ^{210}Pb results in an "excess" of ^{210}Pb (^{210}Pb$_{ex}$) relative to the levels supported by the direct decay of ^{222}Rn. As surface sediments are eroded into a river, channel sediments become enriched in ^{210}Pb$_{ex}$. If these channel sediments are subsequently deposited into a floodplain, the floodplain sediments become enriched with ^{210}Pb$_{ex}$. As the rate of floodplain sedimentation decays with increasing distance from the channel, so too should the enrichment of ^{210}Pb$_{ex}$ inventories in floodplain sediment.

If the uniform atmospheric deposition rate D is constant and the vertical accretion caused by overbank deposition decreases exponentially with increasing distance from the channel edge, then the trend toward decreased ^{210}Pb$_{ex}$ inventories $N(x,t)$ with greater distance from the edge of the channel can be quantified as

$$\frac{\partial N(t,x)}{\partial t} = D + \delta_o n_s \rho_s \exp\left(-\frac{x}{x_o}\right) - \lambda N(t) \quad (1)$$

where δ_o is the vertical accretion rate at the channel edge, n_s the isotopic activity of freshly-deposited overbank sediment having a bulk density ρ_s, and x_o is the characteristic distance over which overbank deposition decays away from the channel. We neglect any spatial variation in the initial activity of overbank sediment.

Defining the sediment radionuclide loading rate as

$$\alpha_o = \delta_o n_s \rho_s \quad (2)$$

the total inventory can be written

$$N(t,x) = \int_0^t \left[D + \alpha_o \exp\left(-\frac{x}{x_o}\right) - \lambda N\right] dt. \quad (3)$$

Integrating Eq. (3), the steady state ($t \rightarrow \infty$)^{210}Pb$_{ex}$ inventory at any distance x from the edge of the channel is

$$N(x) = \frac{D}{\lambda}\left[1 + \frac{\alpha_o}{D}\exp\left(-\frac{x}{x_\infty}\right)\right]. \quad (4)$$

Implicit in Eq. (4) is the assumption that the channel does not migrate horizontally. This assumption is generally justified for stream systems in the Upper Connecticut River where valleys are relatively confined, channels have low sinuosities, and migration rates are limited (Magilligan et al., 2008; Black et al., 2010).

3. Site descriptions

The West and White rivers are mixed bedrock–alluvium tributaries of the Connecticut River in southern Vermont (Fig. 1); the alluvium in both cases is comprised of gravel and sand. The two watersheds have similar drainage areas and are located within 50 km of each other, so each has similar underlying geology and hydroclimatology. Both watersheds annually receive 115 cm of precipitation more or less uniformly distributed throughout the year, with about one-quarter falling as snow. The average annual temperature is ~7 °C with large seasonal fluctuations.

The mainstem of the White River is unregulated while the mainstem of the West River is regulated by two dams: Ball Mountain Dam and Townshend Dam. This study focuses on three regulated sites on the West River (Fig. 1, Table 1); two below the Ball Mountain Dam and one below Townshend Dam. As points of controlled comparison, we also consider two unregulated sties, one site above Ball Mountain Dam on the West River and one site on the unregulated White River.

3.1. West River

The West River has a watershed area of 1091 km^2 and a mean annual discharge of 10.9 m^3 s^{-1} at the United States Geological Survey (USGS) gage in Jamaica, VT (drainage area = 464 km^2) just below Ball Mountain Dam. The U.S. Army Corps of Engineers completed construction of both the Ball Mountain and Townshend dams on the West River in 1961. Townshend Dam is located 16 km downstream from the Ball Mountain Dam, well below our River Road and Wardsboro brook sites and thus imposing no backwater effects on the main-channel confluences of these locations. The reservoir behind Townshend Dam is the smaller of the two (0.04 km^3) and is maintained at a relatively constant year-round stage reservoir. The larger reservoir behind Ball Mountain Dam (0.104 km^3) extends 7 km above the dam to just below our Winhall River site. The reservoir water depth varies seasonally from 20 m in the spring to 8 m in the summer. The operation of both dams is coordinated primarily for flood control with two weekends of controlled releases from Ball Mountain Dam each year for recreation. Regulation has significantly reduced peak flows on the West River below both dams. Although the average daily flows have been somewhat larger during the post-regulation era than before dam construction, the

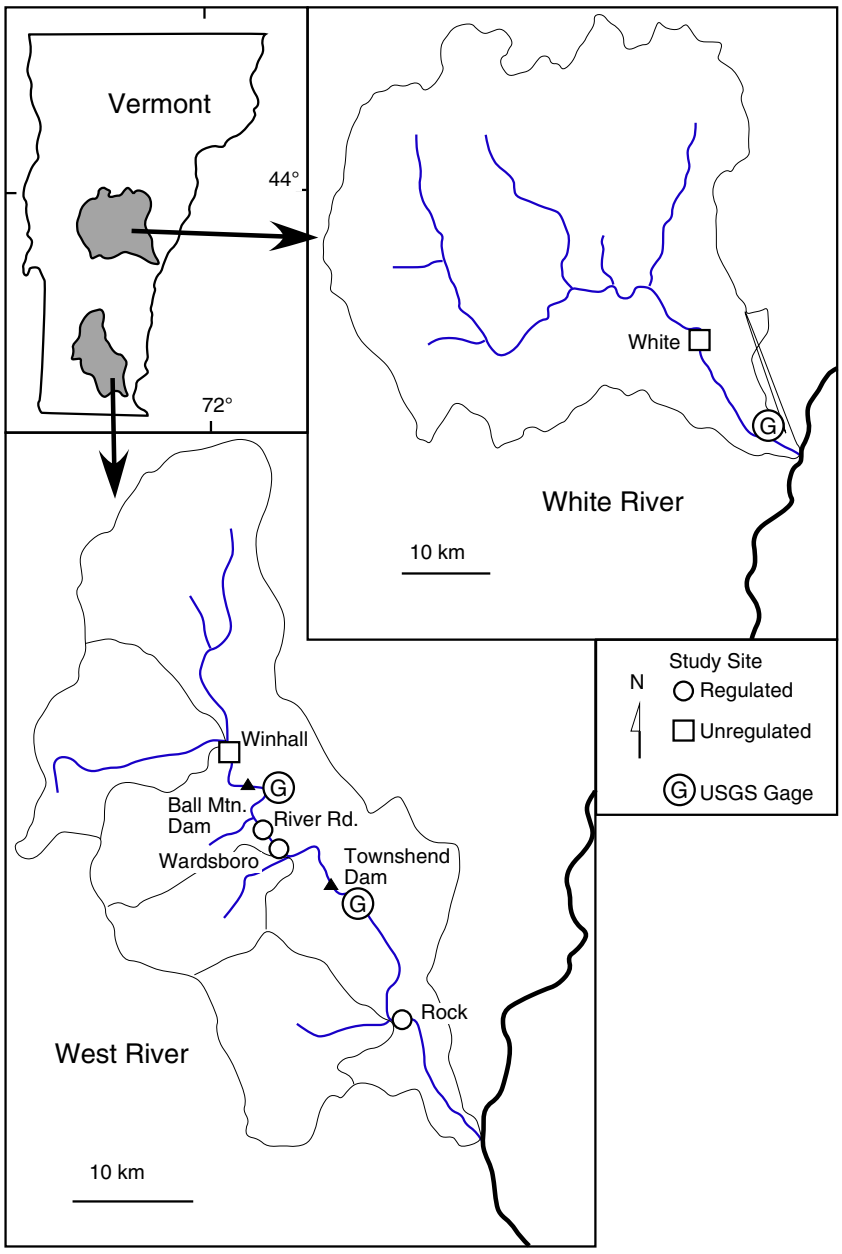

Fig. 1. Locations of study sites and the U.S. Geological Survey gages on the White and West rivers, Vermont.

magnitude of the 50-year flood just below the Ball Mountain Dam has been reduced by an order of magnitude from 1035 $m^3 s^{-1}$ to 167 $m^3 s^{-1}$. As a result, the contemporary 50-year flood is similar in magnitude to the pre-dam 2-year flood and during the post-regulation interval, the pre-dam 2-year flood has not occurred on the West River below the dams (Svendsen et al., 2009).

The sediment trapping efficiencies of the dams are unknown, but likely high given their persistent reservoirs and limited releases. Preliminary results from recent estimates of the volume of sediment stored behind Ball Mountain Dam based on ground penetrating radar transects indicate that sediment is being stored behind the dam at a rate similar to the average erosion rate for northern New England (Kasprak et al., 2008), consistent with the purportedly high sediment trapping efficiency of the dam.

Three regulated sites (River Road, Wardsboro Brook, and Rock River) and one unregulated (Winhall River) site upstream of both dams were established along the West River (Fig. 1, Table 1). All but one of these sites were selected because of the presence of large mid-channel islands. Historical aerial photographs and the presence of large trees at least several decades old growing on the islands indicate that the islands existed prior to the onset of regulation. We focus on stable mid-channel islands because they are less prone to anthropogenic disturbances. Since the onset of regulation there have not been floods of sufficient magnitude to fully inundate any of the islands and thus their near-channel floodplains only receive sediment from the nearby channel and not from flows washing over the island.

At the unregulated Winhall site, three transects were measured across an island located ~600 m below the Winhall River tributary. Two of the regulated sites are located between the Ball Mountain and Townshend dams. Two transects were measured across an island at the River Road site ~1500 m downstream of Ball Mountain Brook, the first tributary entering the West River below Ball Mountain Dam. And two transects were measured upstream of Wardsboro brook, the second tributary entering the West River downstream of Ball Mountain

Table 1
Site characteristics on the White and West rivers.

Site	Drainage area (km^2)	Distance from CT River (km)	Distance from Ball Mountain/ Townshend dam (km)	Q2 ($m^3\ s^{-1}$)	Q50 ($m^3\ s^{-1}$)
West River					
Winhall River	416	55	Unregulated	183	570
River Road	552	40	6.7	135	203
Wardsboro Brook	591	38	8.9	144	207
Rock River	1020	14	32.7/17.6	259	371
White River					
White River	1701	21	Unregulated	501	1470

Dam. Two transects were also measured across an island at the final regulated site located ~100 m downstream of Rock River, the second and largest tributary downstream of Townshend Dam.

3.2. White River

The White River drains into the Connecticut River about 50 km above the West River and has a watershed area of 1843 km^2 (Fig. 1). The mean annual discharge is 34.1 $m^3\ s^{-1}$ at the USGS gage station in West Hartford, VT (drainage area = 1787 km^2). One site was selected along the White River, approximately 1 km upstream of the USGS gage. Two transects were measured across a mid-channel island at this site. This site complements our other unregulated site upstream of the dams on the West River.

4. Methods

4.1. Channel and sediment profiles

Topographic surveys along transects perpendicular to the river channel were measured using a Topcon *Hiper Lite* + real-time differential GPS. The accuracy of the GPS survey was ~2 cm, except along the channel banks where trees interfered with satellite communication. An optical auto level or rotating leveling laser with laser detectors attached to a stadia rod was used to determine bank elevation in areas with poor satellite reception.

Sediment profiles were collected at relatively flat terraces separated by significant elevation differences along each transect. Two to four profiles were collected along each transect. Profiles were initially excavated below a 15 cm × 15 cm template to a depth of 30 cm and samples collected in three increments; 0–5 cm, 5–15 cm, and 15–30 cm. Deeper soil samples, up to a depth of 90 cm, were collected in 20-cm increments using a 5-cm I.D. piston corer. The collected sediments were stored in plastic bags for transport to the laboratory.

After collection, all samples were oven dried for a minimum of 2 days at 60 °C. Samples were then homogenized before being tightly packed into uniform-sized plastic containers (105 mL) with masses ranging from 57 to 218 g. To measure ^{210}Pb and ^{226}Ra activity, Canberra Intrinsic High Purity Germanium Detectors were used to quantify gamma ray emissions from the samples. Total ^{210}Pb activity was determined from gamma ray emissions measured at 46 keV. ^{226}Ra activity was determined using the ^{214}Pb gamma ray emission at 352 keV after the sample had been sealed for 3 weeks. Excess $^{210}Pb_{ex}$ activity was determined by subtracting ^{226}Ra activity from the total ^{210}Pb activity.

Detector efficiency was determined by spiking representative samples with a certified uranium ore. In order to account for the low photon energy of the ^{210}Pb gamma emission, a self-attenuation correction was made for each sample by measuring gamma ray transmission through each sample from a ^{210}Pb point source on top of the sample.

The two primary sources of measurement error involved in measuring the activity of ^{210}Pb via gamma spectroscopy are the uncertainty inherent in photon emission statistics and in background subtraction. The uncertainty inherent in photon emission statistics is directly related to the total number of decays or counts (n) recorded by the detector, where $\sigma_n = \sqrt{n}$. All samples were run until they accumulated between 750 and 1250 ^{210}Pb counts. The uncertainty from background subtraction was determined using the uncertainty of a linear fit of the spectral data surrounding the photopeak.

4.2. Flow modeling

To determine the recurrence interval of the discharges required to inundate the surface associated with each sediment profile, the Army Corps of Engineers flow modeling program HEC-RAS was used to model flow at each transect. A normal depth boundary condition was used along the furthest downstream transect by approximating the energy grade slope as equal to the downstream water surface gradient during cross-sectional surveys. Typical values of Manning's n of 0.04 for the channel and 0.08 for the channel banks were assumed. Reducing the channel and floodplain roughness to 0.03 and 0.07, respectively, to accommodate roughness decreases commonly observed with high stages (Barnes, 1967; Hicks and Mason, 1991; Magilligan, 1992) had no significant impact on model results.

The recurrence interval for each modeled discharge was determined by extrapolating annual peak discharges observed at nearby USGS gage stations using the Vermont regional discharge curve (Jaquith and Kline, 2001). Flood recurrences were estimated assuming a Log Pearson type III distribution.

Annual peak discharges at the regulated River Road and Wardsboro sites were extrapolated from the post-dam annual peak discharges observed between 1961 and 2009 at the USGS gage station below Ball Mountain Dam near Jamaica, VT (USGS gage 01155500). Annual peak discharges for the regulated Rock River site were extrapolated from the post-dam annual peak discharges observed between 1961 and 1995 at the USGS gage station below Townshend Dam near Newfane, VT (USGS gage 01156000). Annual peak discharges for the unregulated Winhall site were extrapolated from the annual peak discharges recorded between 1940 and 2009 at the nearby USGS gage on the unregulated Saxtons River near Saxtons River, VT (USGS gage 01154000). Finally, discharges for the unregulated White River site were assumed equal to those recorded between 1915 and 2009 at the USGS gage on the White River in West Hartford, VT (USGS gage 01144000). No tributaries enter the White River between the gage at West Hartford sampling site located 1 km upstream from the gage.

5. Results

5.1. Inventory versus distance across floodplain

The variation in $^{210}Pb_{ex}$ inventories shown in Fig. 2 for the River Road site is typical of those observed at all the sites. In the first panel the $^{210}Pb_{ex}$ inventory is plotted as function of the horizontal distance from the nearest water surface when the discharge is equal to the mean annual flow, shown as the shaded region in the topographic profiles in panels b) and c). The letters next to the $^{210}Pb_{ex}$ inventories indicate the locations of the sediment inventories along the topographic profiles.

Fig. 2 demonstrates two findings that are observed at all regulated and unregulated sites. First, there is no consistent variation in $^{210}Pb_{ex}$ inventory with distance from the mean annual water surface. This likely reflects the asymmetry of the topographic profiles. Consider, for example, sediment profiles C and E; both are located ca. 20 m from the mean annual water surface, yet the $^{210}Pb_{ex}$ inventory of profile C is more than 50% greater than that of profile E. The difference in inventories is likely due to the greater inundation frequency at site C, which is

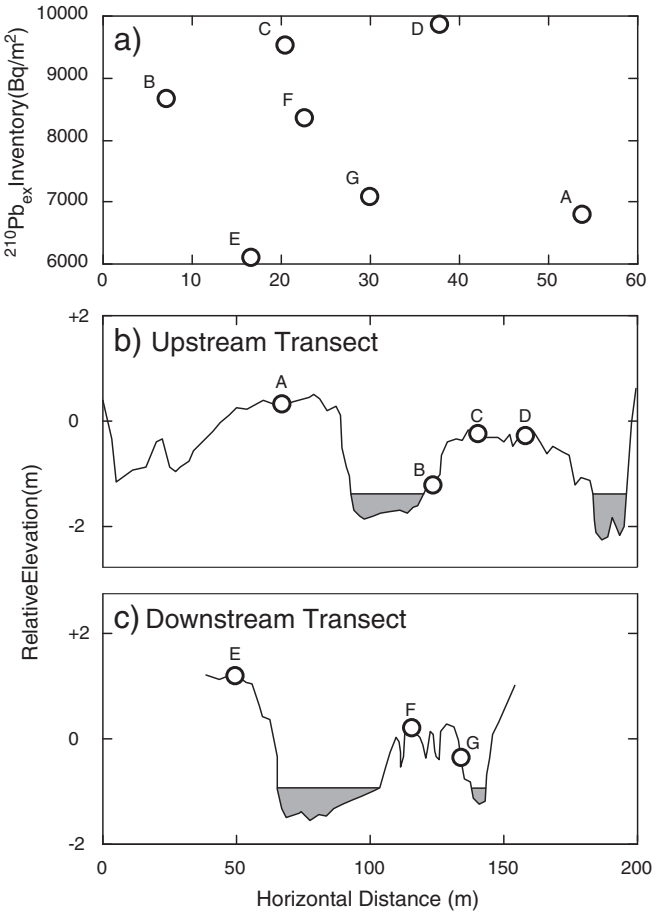

Fig. 2. a) Variation in $^{210}Pb_{ex}$ inventories at the River Road site with distance from the mean annual flow. Letters next to each inventory correspond to the sampling location shown on the b) upstream (with respect to the other profile) and c) downstream topographic profiles. Shaded regions on topographic profiles correspond to stage associated with the mean annual flow. See main text for discussion.

only ca. 1-m above the mean annual water surface, about half as high as profile E. This suggests at sites such as ours where floodplains are narrow and have significant topography, inundation frequency, or recurrence interval for flooding, may be a better independent metric than linear distance for comparing $^{210}Pb_{ex}$ inventories across different channel banks. Moody et al. (1999) have noted that as a floodplain aggrades, the recurrence interval for flooding at a specific location will increase and thus, at a given location, is not constant over time. However, because of the granitic terrain of New England and recent glacial history, New England rivers are characterized by suspended sediment concentrations that are among the lowest in the U.S. (Rainwater, 1962). Consequently, aggradation rates at our sites are likely low (more below) and, in most cases, the recurrence interval for flooding is nearly constant over the decadal time scale considered here. Also, while at specific sites vertical river stage and inundation frequency are related, this relationship is transect specific. Thus recurrence interval for flooding is a better independent metric than vertical stage for comparing inventories across different transects.

Also apparent in Fig. 2, and typical of our other profiles, the highest $^{210}Pb_{ex}$ inventories do not occur closest to the mean annual water surface. For example, at River Road, the $^{210}Pb_{ex}$ inventory is greater in profile C than in profile B, even though profile B is closer to the mean annual water surface. This contrast is consistent with the results from flume studies by Bathurst et al. (2002) who found that peak overbank sedimentation did not occur at the channel edge, but rather at some distance away from the edge of the channel, with peak sedimentation occurring at further distances from the channel edge with larger channel flows. Most likely overbank flow velocities immediately adjacent to the channel are too high to permit significant sediment deposition during high water and may even erode previously deposited sediments.

These observations suggest two modifications to the conceptual model for the variation in radionuclide inventories presented in Eq. (4). First, rather than expressing the decay in deposition as a function of distance from the channel, it may be better instead to define this decay as a function of recurrence interval for flooding. Using flooding frequency rather than distance from the channel as the independent variable represents a time-for-space, or more precisely, frequency-for-space, substitution for the independent variable controlling floodplain $^{210}Pb_{ex}$ inventories. Also, as noted earlier, and consistent with field observations, we assume that the channel is not migrating. Secondly, because peak $^{210}Pb_{ex}$ inventories do not occur at the channel edge, the decay in deposition should be expressed as a function of the offset from the location of the peak inventory rather than from the channel edge. Thus our modified model for the variation in $^{210}Pb_{ex}$ inventories is

$$\frac{\partial N(t,R)}{\partial t} = D + \delta_o n_s \rho_s \exp\left(-\frac{R-R_{pk}}{R_\infty}\right) - \lambda N(t) \qquad \frac{R-R_{pk}}{R_\infty} \geq 0 \tag{5}$$

where R_{pk} is the recurrence interval for flooding of the profile having the greatest $^{210}Pb_{ex}$ inventory and R_∞ is the characteristic difference in inundation frequency over which overbank deposition decays. Integrating Eq. (5), the steady state ($t \to \infty$) total radionuclide inventory for a given recurrence interval is

$$N(R) = \frac{D}{\lambda}\left[1 + \frac{\alpha_o}{D}\exp\left(-\frac{R-R_{pk}}{R_\infty}\right)\right] \qquad \frac{R-R_{pk}}{R_\infty} \geq 0. \tag{6}$$

To facilitate the comparison of different sites, we define the dimensionless $^{210}Pb_{ex}$ inventory N_D and relative recurrence internal R_D as

$$N_D = \frac{N(R)-N_{eq}}{N_{pk}-N_{eq}}, \qquad R_D = \frac{R-R_{pk}}{R_\infty} \tag{7,8}$$

where the peak and equilibrium atmospheric $^{210}Pb_{ex}$ inventories are defined as

$$N_{pk} = \frac{1}{\lambda}(D + \alpha_o), \qquad N_{eq} = \frac{D}{\lambda}. \tag{9,10}$$

Substituting Eqs. (7–10) into Eq. (6) yields

$$N_D = \exp(-R_D) \qquad R_D \geq 0. \tag{11}$$

To apply this model to our $^{210}Pb_{ex}$ data, we first note that $N(R \to \infty) = D/\lambda = N_{eq}$. Thus at each site we approximate N_{eq} as equal to the inventory of the sediment profile having the highest recurrence interval (Table 2). The average equilibrium inventory of all sites of 6120 ± 310 Bq m^{-2} (mean ± S.E.) agrees well with the inventories measured by Kaste et al. (2003) for deciduous forests in northern Vermont (6510 ± 890 Bq m^{-2}) and corresponds to an atmospheric deposition rate D = 202 ± 28 Bq m^{-2} yr^{-1}. Similarly, the peak inventory, N_{pk}, is approximated as equal to the inventory corresponding to R_{pk} (Table 2). Finally, we use multiparameter optimization (Press et al., 1992) to determine the value of R_∞ that provides the least squares best fit of Eq. (11) to the inventories along the transect for which $R \geq R_{pk}$ (Table 2).

Fig. 3 compares variation in measured inventories to that predicted by Eq. (11). Overall the fit to the model is good, demonstrating a surprising similarity in the variation in the overbank depositional profiles across regulated and unregulated sites.

Table 2
Parameters of the depositional profiles.

Site	N_{eq} (Bq m^{-2})	N_{pk} (Bq m^{-2})	R_{pk} (yr)	R_∞[a] (yr)	Channel sediment $^{210}Pb_{ex}$ (Bq/kg)	Surface $^{210}Pb_{ex}$ at R_{pk} (Bq/kg)	δ_o (mm yr^{-1})
Regulated							
River Road	6118	9875	2.5	3.3 ± 0.9	10.6	48.5	2–7
Wardsboro	6559	15,266	1.1	0.4 ± 0.06	14.0	57.7	3–13
Rock River	5730	6625	1.1	0.4 ± 0.02	1.8	22.9	1–10
Unregulated							
Winhall	6970	9371	1.5	0.4 ± 0.1	8.1	45.7	1–6
White	5220	11,542	3.9	1.2 ± 0.01	3.0	28.6	5–44

[a] Best fit ± σ to Eq. (11).

Combining Eqs. (2, 9, and 10), the vertical accretion rate δ_o is related to the peak and equilibrium inventories as

$$\delta_o = \frac{\lambda\left(N_{pk} - N_{eq}\right)}{n_s \rho_s}. \quad (12)$$

Thus converting the measured inventories shown in Fig. 3 to vertical accretion rates requires the initial isotopic activity of the overbank sediment n_s. A lower bound estimate for this activity is provided by the measured isotopic activity of fine (<2 mm) channel bed sediment immediately upstream of the sediment profiles (Table 2). Corresponding upper bound estimates of sediment deposition rates at our sites are ca. cm yr^{-1} (Table 2). These rates are unrealistically high in that if sediments were being deposited this quickly we would expect a topographic expression of the high rates of sedimentation at R_{pk} such as a berm or levee. Additionally, we would expect a closer correspondence between the activity of the fine sediment in the channel and the activity of the near surface sediment at R_{pk}. Although the activity of the channel bed and the activity of the near surface sediment at R_{pk} are highly correlated ($r^2 = 0.98$), the activity of the near surface sediment at R_{pk} is consistently greater than that of the fine sediment in the channel (Table 2).

It follows that a lower bound estimate of the sedimentation rate is given by the activity of the near surface sediment at R_{pk} (Table 2). This is a lower bound estimate because the activity of near surface sediment reflects input both from overbank sedimentation and also atmospheric deposition. Corresponding lower bound estimates of sediment deposition rates at our sites are a few mm yr^{-1} (Table 2). Although low, these rates are still two orders of magnitude greater than the average denudation rate in New England (Gordon, 1979; Kasprak et al., 2008) and similar to those measured elsewhere (Magilligan, 1985; Keesstra, 2007; Pierce and King, 2008; Humphries et al., 2010; Lokas et al., 2010; Saint-Laurent et al., 2010; Wallinga et al., 2010). Within the accuracy of our estimates there is no discernable difference in sedimentation rate between our regulated and unregulated sites.

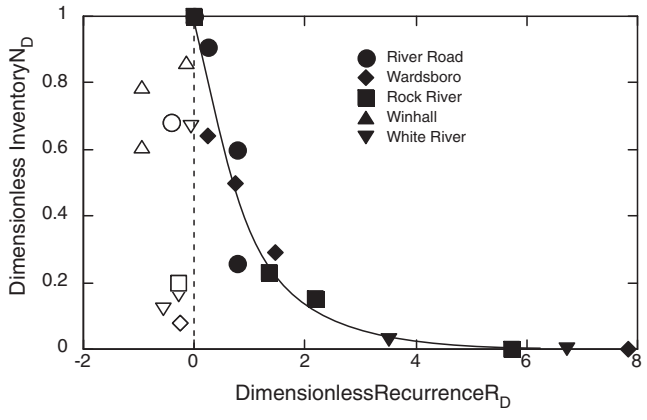

Fig. 3. Variation in normalized $^{210}Pb_{ex}$ inventories as a function of normalized recurrence interval for flooding. Solid line indicates variation predicted by Eq. (11) as fit using the data indicated by filled symbols. Dashed line is for reference and indicates where R_D is equal to zero.

6. Discussion

6.1. Controls on depositional profile

$^{210}Pb_{ex}$ inventories show a consistent pattern of variation across all regulated and unregulated sites. Inventories are low immediately adjacent to the channel where the overbank flows are common, but increase rapidly to a peak value before decreasing asymptotically to approach the equilibrium inventory for atmospheric deposition. Inventories in excess of the equilibrium inventory for atmospheric deposition are proportional to the rate of overbank sedimentation and also the activity of the deposited sediment, which appears to vary from site to site but is likely greater than the activity of in-channel sediment. Accordingly, the low inventories immediately adjacent to the channel are due to low rates of overbank sedimentation in this zone, most likely because flow velocities during floods in this region are too great to permit the settling of sediment. As flow velocities and the frequency of inundation decrease away from the channel, the rate of overbank sediment deposition increases rapidly and then peaks. In systems where the rate of overbank sediment deposition is large, the peak in deposition rate will create the commonly observed natural levees along channel banks (e.g., Pizzuto et al., 2008). That natural levees are not apparent at our sites is likely due to their low sediment deposition rates. Beyond the region of greatest sediment deposition, the rate of sediment deposition apparently decreases exponentially with decreasing inundation frequency. Although this general pattern of variation in sediment deposition is present at all sites, both the location of the peak in sediment deposition, R_{pk}, and the characteristic scale over which sediment deposition decreases with decreasing inundation frequency, R_∞, vary between sites. However, the variation in these parameters is not systematic with degree of flow regulation.

6.2. Impact of regulation

While the similarity in sediment deposition profiles between regulated and unregulated reaches shown by Fig. 3 indicates a similarity in depositional processes across these sites, it does not imply that regulation has not impacted floodplain sedimentation. Consider, for example, the floodplain at the Wardsboro site (Fig. 1). If R_{pk}, R_∞ and δ_o each remained unchanged after the onset of regulation, net sedimentation to the floodplain at this site has decreased post regulation. This pattern is shown in Fig. 4 which compares sediment deposition rates before and after regulation. Here sediment deposition is normalized by the peak sediment deposition rate δ_o. The difference in profiles is due to the reduction in frequency of flood events with the onset of regulation. For example, the 2-year flood at this site decreased 50%

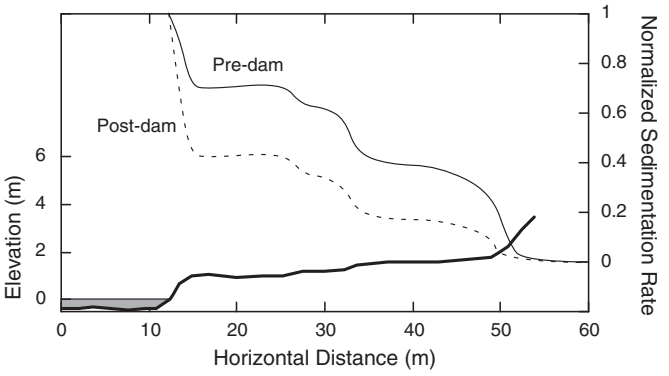

Fig. 4. Comparison of depositional profiles at the Wardsboro site before (thin solid line) and after (dashed line) the onset of flow regulation. Deposition rates are normalized by the peak deposition rate. Bold line represents the topographic profile.

from 238 $m^3\ s^{-1}$ to 144 $m^3\ s^{-1}$. The decrease in size of larger flood events was even greater. For example, the 50-year flood event decreased more than 80% from 1200 $m^3\ s^{-1}$ to 200 $m^3\ s^{-1}$. Because the form of the deposition profile depends on the frequency of inundation rather than distance from the channel, the reduction in magnitude of the high flow events also reduced the spatial extent of the deposition (Fig. 4). Thus even if the rate of peak deposition remained constant, total deposition on the floodplain decreases by ca. 20% with the onset of regulation due to the decreased frequency of inundation.

7. Conclusions

Detailed mapping of overbank deposits from individual events (Middelkoop and Asselman, 1998) as well as detailed models of overbank hydraulics and sediment transport and deposition (Nicholas and Walling, 1998; Nicholas and Mitchell, 2003) have highlighted the important role of local-scale topographic features such as levees and abandoned channels on overbank sedimentation (Nicholas et al., 2006). Despite these potential local-scale complexities, we find remarkably consistent profiles of $^{210}Pb_{ex}$ inventories across all our sites; inventories are lowest immediately next to the channel, increase to a peak value as the inundation frequency decreases and then asymptotically diminish with distance from the channel (in recurrence interval space) to the equilibrium inventory associated with atmospheric deposition alone. That we do not observe significant disruptions to this pattern associated with local-scale topography may reflect the relatively long time-scale represented by the $^{210}Pb_{ex}$ inventory, the relative stability of our channels, and/or the low rates of overbank sedimentation.

As expected, we infer from our data that flow regulation has impacted sediment deposition to floodplains below the dam; total sediment deposition is less and it is constrained to a narrower band immediately along the active channel. Flow regulation does not appear, however, to impact the general form of the $^{210}Pb_{ex}$ inventory profile, suggesting a uniformity of process across regulated and unregulated floodplains. Regulation appears not to change the dynamics of near-channel floodplain sedimentation, but instead focuses deposition across a narrower band of the floodplain due to the compression of the differences in size between small and large floods and their corresponding floodplains. In other words, rates of overbank deposition at both our regulated and unregulated sites are principally controlled by inundation frequency regardless of the degree of flow regulation. To the extent that regulation alters flood recurrence, so too will floodplain deposition be impacted.

Acknowledgments

This work was partially supported by the U.S. National Science Foundation (BCS-0724348) and in part with support from The Nature Conservancy (Connecticut River Research Partnership Agreement).

References

Allred, T.M., Schmidt, J.C., 1999. Channel narrowing by vertical accretion along the Green River near Green River, Utah. Geological Society of America Bulletin 111 (12), 1757–1772.
Andrews, E.D., 1986. Downstream effects of Flaming Gorge Reservoir on the Green River, Colorado and Utah. Geological Society of America Bulletin 97 (8), 1012–1023.
Appleby, P.G., 2008. Three decades of dating recent sediments by fallout radionuclides: a review. The Holocene 18 (1), 83–93.
Appleby, P.G., Oldfield, F., 1992. Application of 210-Pb to sedimentation studies. In: Invanovich, M., Harman, R.S. (Eds.), Uranium-series Disequilibrium: Application to Earth, Marine, and Environmental Sciences. Clarendon Press, Oxford, UK, pp. 731–778.
Asselman, N.E.M., Middelkoop, H., 1995. Floodplain sedimentation — quantities, patterns and processes. Earth Surface Processes and Landforms 20 (6), 481–499.
Barnes, H.H., 1967. Roughness characteristics of natural channels. U.S. Geological Survey Water Supply Paper, 1849.
Bathurst, J.C., Benson, I.A., Valentine, E.M., Nalluri, C., 2002. Overbank sediment deposition patterns for straight and meandering flume channels. Earth Surface Processes and Landforms 27 (6), 659–665. http://dx.doi.org/10.1002/esp.346.
Black, E.E., Renshaw, C.E., Magilligan, F.J., Kaste, J.M., Dade, W.B., Landis, J.D., 2010. Determining lateral migration rates using fallout radionuclides. Geomorphology 118 (1–2), 105–117.
Bornette, G., Amoros, C., Piegay, H., Tachet, J., Hein, T., 1998. Ecological complexity of wetlands within a river landscape. Biological Conservation 85 (1–2), 35–45.
Bourgoin, L.M., Bonnet, M.P., Martinez, J.M., Kosuth, P., Cochonneau, G., Moreira-Turcq, P., Guyot, J.L., Vauchel, P., Filizola, N., Seyler, P., 2007. Temporal dynamics of water and sediment exchanges between the Curuai floodplain and the Amazon River, Brazil. Journal of Hydrology 335 (1–2), 140–156. http://dx.doi.org/10.1016/j.jhydrol.2006.11.023.
Cavalcanti, G.G., Lockaby, B.G., 2005. Effects of sediment deposition on fine root dynamics in riparian forests. Soil Science Society of America Journal 69 (3), 729–737. http://dx.doi.org/10.2136/sssaj2004.0239.
Connell, J.H., 1978. Diversity in tropical rain forests and coral reefs — high diversity of trees and corals is maintained only in a non-equilibrium state. Science 199 (4335), 1302–1310.
Curtis, K.E., Renshaw, C.E., Magilligan, F.J., Dade, W.B., 2010. Temporal and spatial scales of geomorphic adjustments to reduced competency following flow regulation in bedload dominated systems. Geomorphology 118 (1–2), 105–117.
Day, G., Dietrich, W.E., Rowland, J.C., Marshall, A., 2008. The depositional web on the floodplain of the Fly River, Papua New Guinea. Journal of Geophysical Research — Earth Surface 113 (F1). http://dx.doi.org/10.1029/2006jf000622 (F01s02).
Debano, L.F., Schmidt, L.J., 1990. Potential for enhancing riparian habitats in the southwestern United States with watershed practices. Forest Ecology and Management 33–4 (1–4), 385–403.
Friedman, J.M., Osterkamp, W.R., Scott, M.L., Auble, G.T., 1998. Downstream effects of dams on channel geometry and bottomland vegetation: regional patterns in the Great Plains. Wetlands 18 (4), 619–633.
Gaeuman, D., Schmidt, J.C., Wilcock, P.R., 2005. Complex channel responses to changes in stream flow and sediment supply on the lower Duchesne River, Utah. Geomorphology 64 (3–4), 185–206. http://dx.doi.org/10.1016/j.geomorph.2004.06.007.
Gordon, R.B., 1979. Denudation rate of central New England determined from estuarine sedimentation. American Journal of Science 279 (6), 632–642.
Grams, P.E., Schmidt, J.C., 2002. Streamflow regulation and multi-level floodplain formation: channel narrowing on the aggrading Green River in the eastern Uinta Mountains, Colorado and Utah. Geomorphology 44 (3–4), 337–360.
Grams, P.E., Schmidt, J.C., Topping, D.J., 2007. The rate and pattern of bed incision and bank adjustment on the Colorado River in Glen Canyon downstream from Glen Canyon Dam, 1956–2000. Geological Society of America Bulletin 119 (5–6), 556–575. http://dx.doi.org/10.1130/b25969.1.
Grime, J.P., 1973. Competitive exclusion in herbaceous vegetation. Nature 242 (5396), 344–347.
He, Q., Walling, D.E., 1996. Use of fallout Pb-210 measurements to investigate longer-term rates and patterns of overbank sediment deposition on the floodplains of lowland rivers. Earth Surface Processes and Landforms 21 (2), 141–154.
Henry, C.P., Amoros, C., 1995. Restoration ecology of riverine wetlands 1. A scientific base. Environmental Management 19 (6), 891–902.
Hicks, D.M., Mason, P.D., 1991. Roughness characteristics of New Zealand rivers. New Zealand Water Resources Survey.DSIR Marine and Freshwater, Wellington (329 pp.).
Humphries, M.S., Kindness, A., Ellery, W.N., Hughes, J.C., Benitez-Nelson, C.R., 2010. ^{137}Cs and ^{210}Pb derived sediment accumulation rates and their role in the long-term development of the Mkuze River floodplain, South Africa. Geomorphology 119, 88–96.
Jaquith, S., Kline, M., 2001. Vermont stream geomorphic assessment: Vermont hydraulic geometry curves. River Management Program.Vermont Quality Division, Vermont Agency of Natural Resources, Montpelier.
Kasprak, A., Arcone, S.A., Dade, W.B., Finnegan, D.C., Magilligan, F.J., Renshaw, C.E., 2008. Using ground-penetrating radar to estimate sediment accumulation in a reservoir: Ball Mountain Dam, West River, Vermont. Eos Trans. Amer. Geophys. Union Suppl., 89, pp. H53B–H1044B.
Kaste, J.M., Friedland, A.J., Sturup, S., 2003. Using stable and radioactive isotopes to trace atmospherically deposited Pb in montane forest soils. Environmental Science & Technology 37 (16), 3560–3567.
Keesstra, S.D., 2007. Impact of natural reforestation on floodplain sedimentation in the Dragonja basin, SW Slovenia. Earth Surface Processes and Landforms 32 (1), 49–65. http://dx.doi.org/10.1002/esp.1360.
Lambert, C.P., Walling, D.E., 1987. Floodplain sedimentation — a preliminary investigation of contemporary deposition within the lower reaches of the river Culm, Devon, UK. Geografiska Annaler. Series A, Physical Geography 69 (3–4), 393–404.

Lokas, E., Wachniew, P., Ciszewski, D., Owczarek, P., Chau, N.D., 2010. Simultaneous use of trace metals, Pb-210 and Cs-137 in floodplain sediments of a lowland river as indicators of anthropogenic impacts. Water, Air, and Soil Pollution 207 (1–4), 57–71. http://dx.doi.org/10.1007/s11270-009-0119-4.

Lowe, B.J., Watts, R.J., Roberts, J., Robertson, A., 2010. The effect of experimental inundation and sediment deposition on the survival and growth of two herbaceous riverbank plant species. Plant Ecology 209 (1), 57–69. http://dx.doi.org/10.1007/s11258-010-9721-1.

Ludwig, W., Probst, J.L., Kempe, S., 1996. Predicting the oceanic input of organic carbon by continental erosion. Global Biogeochemical Cycles 10 (1), 23–41.

Magilligan, F.J., 1985. Historical floodplain sedimentation in the Galena river basin, Wisconsin and Illinois. Annals of the Association of American Geographers 75 (4), 583–594.

Magilligan, F.J., 1992. Thresholds and the spatial variability of flood power during extreme floods. Geomorphology 5 (3–5), 373–390.

Magilligan, F.J., Nislow, K.H., 2005. Changes in hydrologic regime by dams. Geomorphology 71 (1–2), 61–78. http://dx.doi.org/10.1016/j.geomorph.2004.08.017.

Magilligan, F.J., Haynie, H.J., Nislow, K.H., 2008. Channel adjustments to dams in the Connecticut River basin: implications for forested mesic watersheds. Annals of the Association of American Geographers 98 (2), 267–284.

Mertes, L.A.K., 1994. Rates of floodplain sedimentation on the central Amazon river. Geology 22 (2), 171–174.

Middelkoop, H., Asselman, N.E.M., 1998. Spatial variability of floodplain sedimentation at the event scale in the Rhine–Meuse delta, the Netherlands. Earth Surface Processes and Landforms 23 (6), 561–573.

Moody, J.A., Pizzuto, J.E., Meade, R.H., 1999. Ontogeny of a floodplain. Geological Society of America Bulletin 111 (2), 291–303.

Nicholas, A.P., Mitchell, C.A., 2003. Numerical simulation of overbank processes in topographically complex floodplain environments. Hydrological Processes 17 (4), 727–746. http://dx.doi.org/10.1002/hyp.1162.

Nicholas, A.P., Walling, D.E., 1998. Numerical modelling of floodplain hydraulics and suspended sediment transport and deposition. Hydrological Processes 12 (8), 1339–1355.

Nicholas, A.P., Walling, D.E., Sweet, R.J., Fang, X., 2006. New strategies for upscaling high-resolution flow and overbank sedimentation models to quantify floodplain sediment storage at the catchment scale. Journal of Hydrology 329 (3–4), 577–594. http://dx.doi.org/10.1016/j.jhydrol.2006.03.010.

Petts, G.E., 1984. Sedimentation within a regulated river. Earth Surface Processes and Landforms 9 (2), 125–134.

Pierce, A.R., King, S.L., 2008. Spatial dynamics of overbank sedimentation in floodplain systems. Geomorphology 100 (3–4), 256–268. http://dx.doi.org/10.1016/j.geomorph.2007.12.008.

Pizzuto, J.E., 1987. Sediment diffusion during overbank flows. Sedimentology 34, 301–317.

Pizzuto, J.E., Moody, J.A., Meade, R.H., 2008. Anatomy and dynamics of a floodplain, Powder River, Montana, USA. Journal of Sedimentary Research 78 (1–2), 16–28. http://dx.doi.org/10.2110/jsr.2008.005.

Press, W.H., Teukolsky, S.A., Vetterling, W.T., Flannery, B.P., 1992. Numerical Recipes in C, the Art of Scientific Computing. Cambridge University Press, New York (994 pp.).

Rainwater, F.H., 1962. Stream Composition of the Coterminous United States. Hydrologic Atlas.U.S. Geological Survey, Washington, D.C.

Saint-Laurent, D., Lavoie, L., Drouin, A., St-Laurent, J., Ghaleb, B., 2010. Floodplain sedimentation rates, soil properties and recent flood history in southern Québec. Global and Planetary Change 70, 76–91.

Salant, N.L., Renshaw, C.E., Magilligan, F.J., 2006. Short and long-term changes to bed mobility and bed composition under altered sediment regimes. Geomorphology 76 (1–2), 43–53.

Stanford, J.A., Ward, J.V., Liss, W.J., Frissell, C.A., Williams, R.N., Lichatowich, J.A., Coutant, C.C., 1996. A general protocol for restoration of regulated rivers. Regulated Rivers: Research & Management 12 (4–5), 391–413.

Steiger, J., Tabacchi, E., Dufour, S., Corenblit, D., Peiry, J.L., 2005. Hydrogeomorphic processes affecting riparian habitat within alluvial channel–floodplain river systems: a review for the temperate zone. River Research and Applications 21 (7), 719–737. http://dx.doi.org/10.1002/rra.879.

Surian, N., 1999. Channel changes due to river regulation: the case of the Piave River, Italy. Earth Surface Processes and Landforms 24 (12), 1135–1151.

Surian, N., Cisotto, A., 2007. Channel adjustments, bedload transport and sediment sources in a gravel-bed river, Brenta River, Italy. Earth Surface Processes and Landforms 32 (11), 1641–1656. http://dx.doi.org/10.1002/esp.1591.

Svendsen, K.M., Renshaw, C.E., Magilligan, F.J., Nislow, K.H., Kaste, J.M., 2009. Flow and sediment regimes at tributary junctions on a regulated river: impact on sediment residence time and benthic macroinvertebrate communities. Hydrological Processes 23, 284–296.

Thoms, M.C., 2003. Floodplain–river ecosystems: lateral connections and the implications of human interference. Geomorphology 56 (3–4), 335–349. http://dx.doi.org/10.1016/s0169-555x(03)00160-0.

Tornqvist, T.E., Bridge, J.S., 2002. Spatial variation of overbank aggradation rate and its influence on avulsion frequency. Sedimentology 49 (5), 891–905.

Vericat, D., Batalla, R.J., 2005. Sediment transport in a highly regulated fluvial system during two consecutive floods (lower Ebro River, NE Iberian Peninsula). Earth Surface Processes and Landforms 30 (4), 385–402. http://dx.doi.org/10.1002/esp.1145.

Walling, D.E., Fang, D., 2003. Recent trends in the suspended sediment loads of the world's rivers. Global and Planetary Change 39 (1–2), 111–126. http://dx.doi.org/10.1016/s091-8181(03)00020-1.

Walling, D.E., He, Q., 1997. Use of fallout Cs-137 in investigations of overbank sediment deposition on river floodplains. Catena 29 (3–4), 263–282.

Walling, D.E., Owens, P.N., 2003. The role of overbank floodplain sedimentation in catchment contaminant budgets. Hydrobiologia 494 (1–3), 83–91.

Walling, D.E., Owens, P.N., Carter, J., Leeks, G.J.L., Lewis, S., Meharg, A.A., Wright, J., 2003. Storage of sediment-associated nutrients and contaminants in river channel and floodplain systems. Applied Geochemistry 18 (2), 195–220.

Wallinga, J., Hobo, N., Cunningham, A.C., Versendaal, A.J., Makaske, B., Middlekoop, H., 2010. Sedimentation rates on embanked floodplains determined through quartz optical dating. Quaternary Geochronology 5, 170–175.

Walls, R.L., Wardrop, D.H., Brooks, R.P., 2005. The impact of experimental sedimentation and flooding on the growth and germination of floodplain trees. Plant Ecology 176 (2), 203–213.

Ward, J.V., 1998. Riverine landscapes: biodiversity patterns, disturbance regimes, and aquatic conservation. Biological Conservation 83 (3), 269–278.

Ward, J.V., Tockner, K., Uehlinger, U., Malard, F., 2001. Understanding natural patterns and processes in river corridors as the basis for effective river restoration. Regulated Rivers: Research & Management 17 (6), 709.

Whited, D.C., Lorang, M.S., Harner, M.J., Hauer, F.R., Kimball, J.S., Stanford, J.A., 2007. Climate, hydrologic disturbance, and succession: drivers of floodplain pattern. Ecology 88 (4), 940–953.